JACS
JOURNAL OF THE AMERICAN CHEMICAL SOCIETY

Article

pubs.acs.org/JACS

Correlating Sterics Parameters and Diastereomeric Ratio Values for a Multicomponent Assembly To Predict Exciton-Coupled Circular Dichroism Intensity and Thereby Enantiomeric Excess of Chiral Secondary Alcohols

Lei You, Jeffrey S. Berman, Attaporn Lucksanawichien, and Eric V. Anslyn*

Department of Chemistry and Biochemistry, The University of Texas at Austin, Austin, Texas 78712, United States

Supporting Information

ABSTRACT: Linear free energy relationship (LFER) substituent parameters are commonly employed for exploring reaction mechanisms and very recently have been used to guide the design of asymmetric catalysts, but their usage in dynamic covalent chemistry is rare. Herein, the properties of an in situ-generated dynamic multicomponent covalent assembly that creates tris(pyridine) metal complexes incorporating chiral secondary alcohols were explored using LFER-based steric parameters. The diastereomeric ratio (*dr*) of the assembly was correlated with the magnitude of the exciton-coupled circular dichroism (ECCD) induced by chiral alcohols. Charton steric parameters were successfully correlated with the *dr* values. Through the combination of these correlations, both the *dr* and CD intensity were predicted for test alcohols. These correlations were also employed to measure a few new Charton parameters. Finally, the prediction of enantiomeric excess (*ee*) of test samples with various alcohol structures was also successfully achieved. The prediction of spectral properties in advance by using well-established steric parameters is shown to be useful for rapid *ee* screening because the need for calibration curves and enantiomerically enriched samples is avoided.

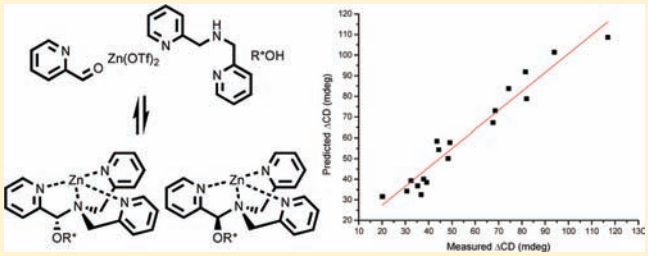

INTRODUCTION

The development of optical sensing approaches for analysis of the absolute configuration and enantiomeric excess (*ee*) of chiral substrates is a major research area in supramolecular analytical chemistry because of their potential applications in asymmetric reaction screening and catalyst development.[1,2] In comparison with GC and HPLC,[3,4] optical techniques are readily adaptable to high-throughput screening of *ee*.[5] Various absorbance-, fluorescence-, and circular dichroism (CD)-based[6−8] supramolecular or reversible covalent approaches have been developed for common chiral building blocks such as amines,[9−11] amino acids,[12,13] carboxylates,[14] 1,2-diamines,[15] 1,2-aminoalcohols,[16] and 1,2-diols.[17,18] Each of these optical assays requires highly enantioenriched samples in advance to create calibration curves that correlate the signal to the *ee*. It would be particularly useful to have a method of predicting the signal achievable by an optical assay, as this would allow its utility to be evaluated before it is implemented. Furthermore, if the signal could be predicted in advance, highly enantiomerically pure samples would not be necessary to train the assay. As a new direction of our longstanding efforts on chirality sensing, we are initiating a project of predicting *ee* values using structural features of the chiral substrates, thereby obviating the need for calibration curves.

The quantitative correlation of reaction thermodynamics and kinetics to linear free energy relationship (LFER)-based electronic or steric substituent parameters is a fundamental concept in physical organic chemistry that has found numerous applications in organic chemistry.[19] For example, the Hammett parameter σ is based on the relative acidity of benzoic acid derivatives to quantify electronic effects (field, induction, and resonance). This parameter and its analogues are routinely employed to elucidate reaction mechanisms.[20,21] Among supramolecular applications, Gokel and co-workers successfully correlated sodium ion transport activity through bilayer membranes with Hammett parameters as a means of probing cation−π interactions.[22]

The Taft steric parameter (E_s) is based on linear free energy relationships of a series of acid-catalyzed reactions, such as hydrolysis of methyl esters (Scheme 1).[23−25] Taft proposed that such a reaction would be minimally affected by electronic effects because the positive charge is maintained from the precursor to the intermediate. However, there has been concern whether steric effects were effectively isolated from polar effects.[26,27] To circumvent these concerns, modified E_s values (υ) based on the van der Waals radii of a specific substituent were proposed by Charton.[28−31] In addition to Taft-type parameters, other steric references, such as Winstein−Holness parameters (*A* values),[32] interference values,[33] and

Received: February 7, 2012
Published: March 22, 2012

dx.doi.org/10.1021/ja3012534 | *J. Am. Chem. Soc.* 2012, 134, 7126−7134

Scheme 1. Acid-Catalyzed Ester Hydrolysis Reaction Used to Derive Taft Parameters and the Related Positive Intermediates

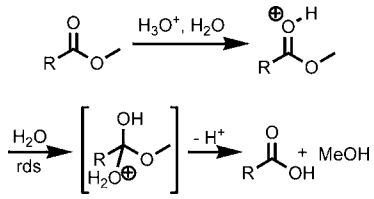

Sterimol parameters,[34] have also been developed and used for various applications. In practice, it is crucial to choose appropriate steric parameters to address specific questions.

Charton υ values have recently been used by Sigman and co-workers to correlate the substituent size of a ligand or a substrate with the logarithm of the enantiomeric ratio (*er*) of various asymmetric catalytic reactions.[35−37] They also employed both Charton and Hammett parameters to design efficient catalysts for an asymmetric propargylation reaction.[38] However, to the best of our knowledge, no such efforts have been made for a multicomponent dynamic process. Catalytic asymmetric reactions generally proceed under kinetic control, and as a result, differences in free energy of the diastereomeric transition states lead to the enantioselectivity. In contrast, dynamic covalent reactions and associated combinatorial libraries are thermodynamically controlled,[39−42] and hence, equilibrium constants rather than rate constants should be employed for correlation and prediction.

In the companion paper (DOI 10.1021/ja301252h), we explored the discrimination of chirality and identity as well as the determination of *ee* of chiral secondary alcohols on the basis of exciton-coupled CD (ECCD) of a dynamic multicomponent covalent assembly (Scheme 2). The assembly of pyridine-2-

Scheme 2. Reversible Multicomponent Covalent Assembly Incorporating a Chiral Alcohol, Leading to a Pair of Diastereomers; the Assembled Complex 1 Was Used as a Sensing Ensemble in ECCD Studies (X Represents Counterions for the Metal Center)

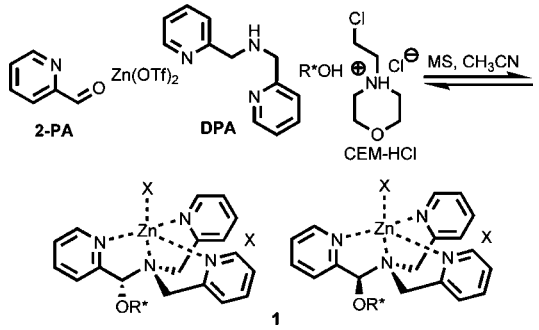

carboxaldehyde (**2-PA**), di(2-picolyl)amine (**DPA**), zinc triflate, and a chiral mono-ol in the presence of molecular sieves and 4-(2-chloroethyl)morpholine hydrochloride (CEM-HCl) as a catalyst[43] gave characteristic diastereomeric ratios (*dr*) as well as CD signals dependent on the structure of the alcohol analyte. In this second paper, we establish theoretical models for quantitatively correlating the CD spectra of the assemblies with the *dr* values, which are also found to correlate with Taft-type steric parameters. These correlations allow us to estimate in advance the CD signals that can be expected for new and previously unexplored alcohols, thereby paving the way for determining *ee* values of unknowns without having purified enantiomers in advance or the need to generate calibration curves.

RESULTS AND DISCUSSION

Model Alcohols. To uncover whether correlations exist between steric parameters and ECCD signals, five chiral alcohols were chosen to span a range of chemical space of groups with different steric features on the α carbon (Scheme 3), including linear alkyl [2-butanol (**BUO**) and 2-octanol

Scheme 3. Structures of the Chiral Secondary Alcohols Studied (Only *R* Stereochemistry Is Shown)

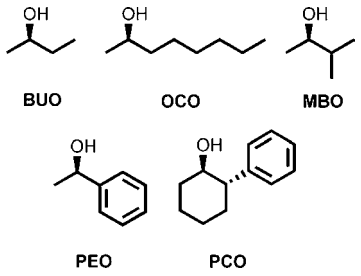

(**OCO**)], branched alkyl [3-methyl-2-butanol (**MBO**)], aromatic [1-phenylethanol (**PEO**)], and cyclic aliphatic [*trans*-2-phenylcyclohexanol (**PCO**)]. The multicomponent assembly reaction was conducted with both enantiomers of each chiral alcohol in the presence of activated 3 Å molecular sieves. The *dr* value is defined as the concentration ratio of the major diastereomer of assembly **1** over the minor diastereomer of **1** at equilibrium for an enantiomerically pure alcohol, and as a result, the *dr* is actually an equilibrium constant and reflects the relative thermodynamic stability of the diastereomers formed. Because of the creation of enantiomeric diastereomers between *R* alcohols and *S* alcohols, they have the same *dr* value. Hence, the *dr* is independent of the *ee* of the alcohol.

The *dr* values for the complexes **1** derived from the five alcohols in Scheme 3 were measured by ^{1}H NMR spectroscopy and ranged between 1.2 and 2.6 (Table 1, column 2). As

Table 1. Values of *dr* and CD Intensity at the First Cotton Effect (268 nm) for *R* Alcohol-Derived Assemblies 1[a]

alcohol	*dr*	CD (mdeg)
BUO	1.30	−20.0
OCO	1.21	−18.4
MBO	1.69	−33.4
PEO	2.18	−40.2
PCO	2.63	−58.6

[a]The assembly reactions were conducted with 35 mM **2-PA** in acetonitrile, and the CD spectra were recorded upon dilution (0.175 mM **2-PA**).

reported in the companion paper, molecular modeling and computational studies revealed that *R* alcohols lead to a preference for an *S* stereocenter at the hemiaminal ether carbon of **1**, which preferentially affords a *P* twist of the three pyridines and a negative CD couplet. Hence, *dr* = [**1**(*S*, *R*)]/[**1**(*R*, *R*)] for *R* alcohols and [**1**(*R*, *S*)]/[**1**(*S*, *S*)] for *S* alcohols, where the first and second letters in the parentheses denote the

dx.doi.org/10.1021/ja3012534 | J. Am. Chem. Soc. 2012, 134, 7126−7134

stereochemistries at the hemiaminal ether carbon and the alcohol α carbon, respectively.

Correlation of CD Magnitude with *dr*. The CD spectra of the assemblies with the various alcohols were recorded and found to be dependent on the alcohol used. The absolute values of signal intensities at the first Cotton effect (268 nm) for these alcohols follow the order **PCO** > **PEO** > **MBO** > **OCO** ≈ **BUO** (Table 1). Table 1 reveals that the *dr* and absolute CD intensity increase together. Hence, the difference in the CD intensities for the *S* and *R* enantiomers of each chiral alcohol at 268 nm (ΔCD) was plotted as a function of the *dr* of the chiral-alcohol-derived complex **1**. A linear correlation was revealed (R^2 = 0.967; Figure 1a and eq 1). This makes intuitive sense because the overall preferential twist in the pyridines should be simply related to the extent of *R* or *S* domination at the hemiaminal ether carbon.

$$\Delta CD = 54.9dr - 30.9 \quad (1)$$

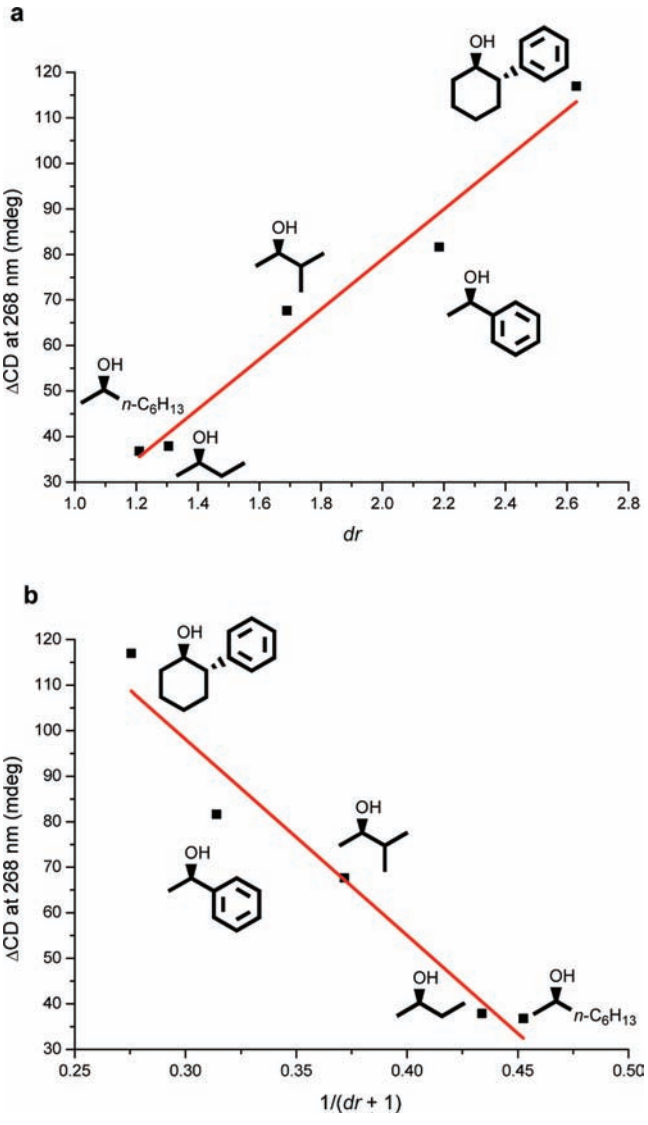

Figure 1. (a) Correlation of ΔCD with *dr* (R^2 = 0.967) (b) Correlation of ΔCD with $1/(dr + 1)$ (R^2 = 0.938). ΔCD is the difference in the CD intensities for the *S* and *R* enantiomers of the alcohol.

Although the linear correlation between the ΔCD and *dr* (Figure 1a) is valid within the range of *dr* used, a perfectly linear relationship is impossible. The CD intensity must reach a maximum plateau when only one diastereomer of assembly **1** is obtained (i.e., as the *dr* approaches infinity), as opposed to an infinite CD magnitude predicted from a purely linear correlation. This inconsistency led to a further examination of the relationship between the CD magnitude and *dr*. As discussed in the companion paper, the alkoxy group plays a minor role in contributing to the ECCD of the assembly **1**, and hence, we can make the assumption that the four diastereomers of **1** have the same absolute value of the CD magnitude at the first Cotton effect. For example, with an enantiomerically pure alcohol (e.g., an *R* alcohol), two diastereomers form: **1**(*S*, *R*) and **1**(*R*, *R*). The two diastereomers afford equal but opposite first Cotton effects, and their concentration ratio is given by the *dr* value. As a result, the overall absolute CD value for an *R*- or *S*-alcohol-derived assembly **1** can be written as shown in eq 2, where |CD| and CD_m are the absolute values for the observed CD magnitude and the CD intensity as *dr* approaches infinity, respectively. These values are the same for *R*- and *S*-alcohol-derived assemblies **1**. The percentages of the major and minor diastereomers are given by $dr/(dr + 1)$ and $1/(dr + 1)$, respectively. Equation 2 can be rearranged to give eq 3. Because ΔCD = 2|CD|, substitution and further rearrangement lead to eq 4, from which a linear correlation between ΔCD and $1/(dr + 1)$ is expected while a hyperbolic relationship between ΔCD and *dr* is apparent (see the Supporting Information for the derivation). This equation also successfully predicts the following: ΔCD = 0 when *dr* = 1 and ΔCD = $2CD_m$ as *dr* approaches infinity.

$$|CD| = CD_m\frac{dr}{dr + 1} - CD_m\frac{1}{dr + 1} \quad (2)$$

$$\frac{|CD|}{CD_m} = \frac{dr - 1}{dr + 1} \quad (3)$$

$$\frac{\Delta CD}{2CD_m} = 1 - \frac{2}{dr + 1} \quad (4)$$

On the basis of eq 4, we plotted ΔCD as a function of $1/(dr + 1)$ and also found a linear correlation (R^2 = 0.938; Figure 1b and eq 5), but with a slightly shallower slope than predicted (1.89 vs 2). This linear correlation predicts that there is a maximum |CD| of 114 mdeg as *dr* approaches infinity. The minimum |CD| of ~6 mdeg is very close to the theoretical value of zero when *dr* approaches 1. The correlation established in Figure 1b is applicable to any possible *dr* value (1 to ∞), while experimentally only a small range of *dr* values was obtained (1.2–2.6) with the alcohols listed in Scheme 3. An approximate linear relationship between ΔCD and *dr* can be obtained over a small range of *dr* using the mathematics of a hyperbolic curve. This explains the origin of the linear fit in Figure 1a.

$$\frac{\Delta CD}{227.3} = 1 - \frac{1.89}{dr + 1} \quad (5)$$

Correlation to Sterics. Having found that the magnitude of the CD spectrum quantitatively correlates with the *dr*, we next turned to correlating the steric features of the alcohol analytes with the *dr* values and CD magnitudes. The differences among the alcohols listed in Scheme 3 are the two groups (except H) attached to the α-carbon. One would predict that the *dr* is dictated by the relative sizes of these two groups

dx.doi.org/10.1021/ja3012534 | J. Am. Chem. Soc. 2012, 134, 7126–7134

(Scheme 3). As a result, steric parameters were employed for the analysis of the *dr* values as well as the CD data.

As described in the Introduction, various steric parameters have been developed. Some of these are derived from experimental measurements, such as Taft-type parameters, while others can be obtained by calculations, such as Sterimol parameters[34] and frontal steric effect-based values.[44,45] In order to use simple and well-known experimental values, Taft-type LFER parameters were chosen. As a result, we used the Charton steric parameters υ for the groups in the chiral alcohols (Table 2) as a means of correlating the sterics with the *dr* and

Table 2. CD Magnitudes, *dr* Values, and Charton Steric Parameters (υ)

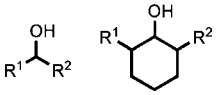

alcohol	*dr*	ΔCD (mdeg)	R^1	$\upsilon(R^1)$	R^2	$\upsilon(R^2)$	$\Delta\upsilon$
PEO	2.18	81.6	Ph	1.66	Me	0.52	1.14
BUO	1.30	37.9	Et	0.56	Me	0.52	0.04
MBO	1.69	67.7	*i*-Pr	0.76	Me	0.52	0.24
PCO	2.63	116.9	Ph	1.66	H	0	1.66

CD values. **OCO** was not used because it gave very similar *dr* and CD values as **BUO**.

Although our multicomponent assembly reaction and the ester hydrolysis shown in Scheme 1 have similar positively charged intermediates, such a similar mechanism is not a prerequisite for using LFER parameters. Actually, Sigman and co-workers demonstrated that the logarithm of the *er* of various asymmetric catalytic reactions with different mechanisms can be correlated with the Charton υ value of a substituent on a ligand or a substrate.[35−38] However, unlike kinetically controlled asymmetric catalytic reactions, our system is under thermodynamic control, and as a result, the equilibrium constants (i.e., *dr* values) were used for the correlation analysis.

There are two values of Charton parameter for the phenyl group (0.57 and 1.66). These values presumably originated from steric interactions above/below (in-plane Ph) or with the edge of the phenyl plane (out-of-plane Ph), respectively. It is worth mentioning that a series of acid-catalyzed reactions, including hydrolysis of esters and esterification of carboxylic acids, were used to derive Taft-type steric parameters. For the reaction in Scheme 1, the extended conjugation of the ester and Ph makes the steric effect of Ph minimal (Scheme 4a). However, for reactions with α-substituted methyl acetate (i.e., RCH_2COOMe), the steric effect of Ph is more pronounced because no such conjugation exists. Presumably, if Ph is perpendicular to the carbonyl in Scheme 1, the nucleophilic attack by water would be most sterically hindered (Scheme 4a). Similarly, in the alcohol substrates studied here, no conjugation with the reaction site (i.e., hydroxyl) is present, and the C−C bond to the Ph can rotate (Scheme 4b). As a result, the out-of-plane Charton value for Ph (1.66) was used in this study. This is supported by the relatively large *dr* value for the **PEO**- and **PCO**-derived assemblies **1**.

Instead of the steric parameter for one substituent, the difference of the Charton parameters ($\Delta\upsilon$) for the two groups on the stereocenter (R^1 and R^2) was applied for acyclic alcohols (Table 2). For cyclic alcohols, we made the assumption that the two groups at positions 2 and 6 of the cyclohexanol play a dominant role in the steric effects because of the rigidity of the

Scheme 4. Rationalization of the Steric Effect of the Phenyl Group with Different Orientations: (a) Newman Projection of Methyl Benzoate Looking Down the C−OMe Bond, Showing In-Plane Ph (left) and Out-of-Plane Ph (right); (b) Newman Projection of *R*-PEO Looking Down the C−OH Bond, Showing In-Plane Ph (left) and Out-of-Plane Ph (right)

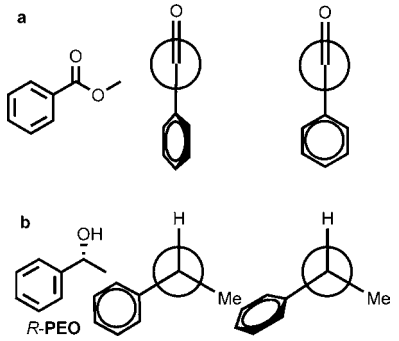

cyclohexane ring relative to acyclic structures. As a result, the two groups at positions 2 and 6 in the cyclohexanol, rather than the two residues on the alcohol stereocenter, were used as R^1 and R^2 (Table 2). Although the groups we are contrasting are one carbon further from the stereocenter in the cyclohexanol cases, the fact that we are using differences between the steric sizes of the groups allows the analysis to work.

The difference in the magnitudes of the ellipticity at 268 nm (ΔCD) varies in accordance with the $\Delta\upsilon$ of the alcohol analyte, and the resultant plot is linear, but with a only modest correlation coefficient (R^2 = 0.834; see the Supporting Information). A much better linear correlation was obtained when the *dr* values were used (R^2 = 0.954; see the Supporting Information). Because $\Delta\upsilon$ values are LFER parameters, it was better to plot log(*dr*) values as a function of $\Delta\upsilon$. This plot was also linear (R^2 = 0.911; Figure 2a and eq 6). This is not surprising because the creation of diastereomers of complex **1** is sterics-sensitive, which is directly reflected in the *dr* values. The fact that both log(*dr*) and *dr* have a linear correlation with $\Delta\upsilon$ arises because only a small range of *dr* values was available (1.2−2.6). It is also worthwhile to mention that multiple linear regression using the υ values of R^1 and R^2 separately afforded eq 7. The similarity of the predictive powers of eqs 6 and 7 is supported by the nearly superimposable *dr* values predicted by these two equations (Figure 2b). This further demonstrated the validity of using $\Delta\upsilon$ for building the model. As discussed in the following sections, the series of linear correlations in Figures 1 and 2 gave us the ability to predict the *dr* and CD magnitude as well as the Charton parameters of substituents whose υ values were not known.

$$\log(dr) = 0.168\Delta\upsilon + 0.145 \quad (6)$$

$$\log(dr) = 0.179\upsilon(R^1) - 0.142\upsilon(R^2) + 0.122 \quad (7)$$

Prediction of *dr* and CD. Once we established a linear relationship between $\Delta\upsilon$ and log(*dr*) (Figure 2), it could be used to predict *dr* values for other alcohols. Several alcohols with diverse structures were chosen to examine the predictive ability of our steric model (Scheme 5): *S*-2-pentanol (**PAO**), *S*-2-hexanol (**HEO**), *R*-1-phenyl-2-propanol (**PPO**), *R*-4-phenyl-2-butanol (**PBO**), and (1*S*,2*R*,5*S*)-(+)-menthol (**MEO**). Their $\Delta\upsilon$ values are listed in Table 3, as well as the predicted *dr* values based upon the relationship shown in Figure 2a and the

dx.doi.org/10.1021/ja3012534 | J. Am. Chem. Soc. 2012, 134, 7126−7134

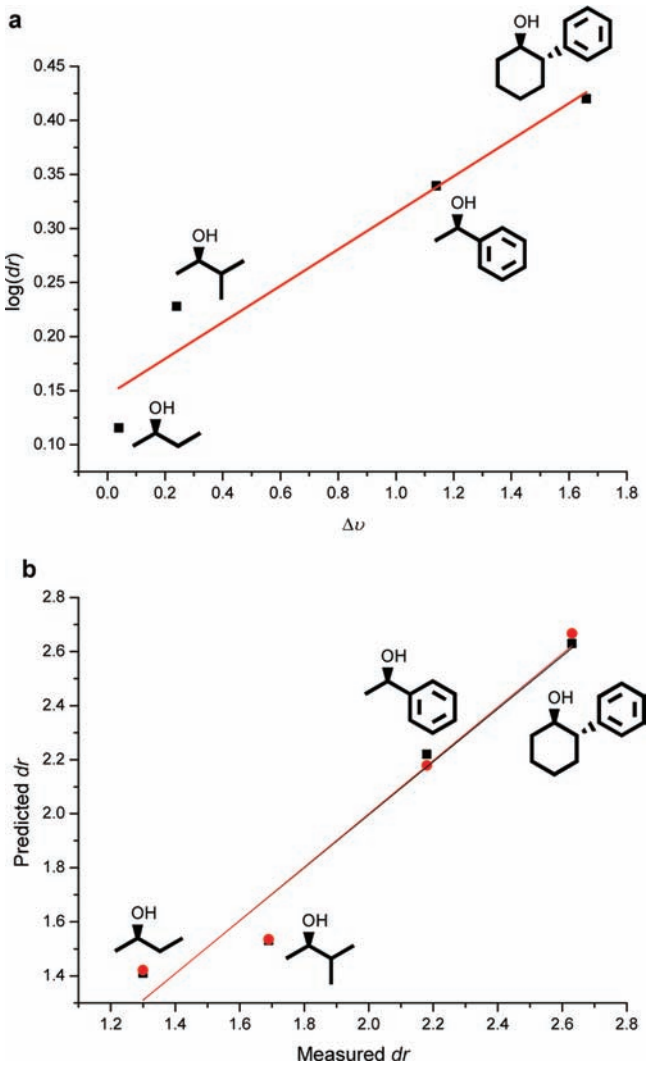

Figure 2. (a) Linear correlation of log(*dr*) with Δυ (R^2 = 0.911). (b) Comparison of measured *dr*, *dr* predicted using eq 6 (red), and *dr* predicted using eq 7 (black). The linear correlation (red) between the measured *dr* and predicted *dr* obtained using eq 6 has a slope of 0.986 (R^2 = 0.941). The linear correlation line (black) between the measured *dr* and predicted *dr* obtained using eq 7 has a slope of 0.979 (R^2 = 0.942). The red and black lines overlap with each other.

Scheme 5. Structures of the Chiral Secondary Alcohols Studied for *dr* and CD Prediction

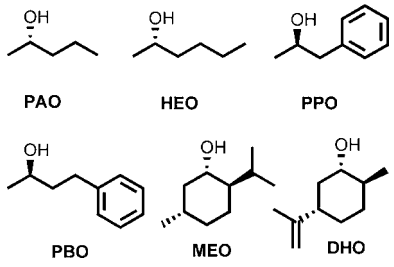

measured *dr* values. As can be gleaned from the table, the measured *dr* values generally correlate well with the predictions. For example, **PAO** and **HEO** have the same Δυ (0.16) and hence the same predicted *dr* (1.49), which closely correlates with their experimental *dr* values (1.28 and 1.26, respectively). It is not surprising that the assembly is relatively insensitive to changes of linear alkyl chains, as evident from the similar *dr* values of **BUO** and **OCO**. Similarly, **PPO** and **PBO** have the same Δυ (0.18) and predicted *dr* values (1.50), but the measured *dr* is higher for **PPO** (1.79) than **PBO** (1.49). This observation is reasonable because we would imagine that benzyl is slightly bulkier than phenylethyl, even if their υ values are the same. For **MEO**, which has 2-propyl and hydrogen on the cyclohexane ring, a calculation with a Δυ of 0.76 gave a *dr* value of 1.88, which is essentially the same as the experimental value (1.90).

After finding success at predicting the *dr* values from the Charton parameters, we turned to predicting the CD data from the Charton parameters. The CD magnitude at 268 nm was predicted from the predicted *dr* value using the linear correlation between *dr* and CD in Figure 1a, and the results are listed in Table 3. Calculation of the predicted CD magnitude using the correlation in Figure 1b gave similar results. Again, the CD intensities predicted solely from Charton values are largely in agreement with the experimental data. **PAO** and **HEO** have similar predicted and experimental CD values (Figure 3). As described above, **PPO** and **PBO** have the same Δυ (0.18) and predicted *dr* (1.50), but the CD magnitude is larger for **PPO** than for **PBO** (Figure 3). For **MEO**, the predicted CD is also comparable to the measured one. Any differences between the CD intensity obtained from the predicted *dr* and the measured CD magnitude are probably due to the accumulation of errors for the two correlations [Δυ to log(*dr*) and *dr* to CD]. This explanation is supported by the CD intensities calculated from the experimental *dr* values, which are very close to the measured CD data.

The predictive power of the correlations was further demonstrated with chiral alcohols whose experimental *dr* values were not available. For example, the *dr* value for the assembly derived from dihydrocarveol (**DHO**; Scheme 5) could not be obtained because of overlap of the ^{1}H NMR peaks. **DHO** is an analogue of **MEO** that has methyl and 2-propene groups at the 2 and 5 positions, respectively. A calculation with a Δυ of 0.52 afforded a *dr* value of 1.71 using eq 6, which is reasonable considering that it is smaller than the experimental *dr* for **MEO** (1.90). A second calculation with the predicted *dr* for **DHO** gave CD magnitudes of 31.4 and 34.3 mdeg using the linear correlations in Figure 1a and Figure 1b, respectively. The predicted CD data are in good agreement with the measured CD intensity for the *S*-**DHO**-derived assembly (37.3 mdeg; see the CD spectra in the companion paper). Hence, the sterics correlations established here using Charton parameters can be used for the prediction of *dr* as well as CD intensity.

Prediction of Charton υ Values. The sterics model was then employed to measure the Charton parameters of other substituents. For *S*-1-(2-naphthyl)ethanol (**NEO**; Scheme 6), the steric parameter for the 2-naphthyl group has not been reported, but a υ value of 1.93 was obtained from the linear correlation using the *dr* value (2.42). In comparison with the value for phenyl (υ = 1.66), the predicted υ value for 2-naphthyl is reasonable because this group is slightly larger. Similarly, on the basis of the *dr* values for *S*-1-(4-fluorophenyl)-ethanol (**FEO**) (*dr* = 2.0) and *S*-1-(2-bromophenyl)ethanol (**BEO**) (*dr* = 1.54), the Charton parameters for 4-fluorophenyl and 2-bromophenyl were found to be 1.44 and 0.77, respectively. It is not surprising that substitution at the para position of Ph has a small effect on the steric size. We would expect ortho substitution to have a much larger effect since it is closer to the reaction site. However, the unfavorable steric

dx.doi.org/10.1021/ja3012534 | *J. Am. Chem. Soc.* 2012, 134, 7126−7134

Table 3. Predicted and Measured *dr* Values and CD intensities at 268 nm; the Correlation in Figure 1a Was Used To Predict CD from *dr*

		dr		CD (mdeg)		
alcohol	$\Delta\upsilon$	predicted *dr*	measured *dr*	predicted[a]	predicted[b]	measured
PAO	0.16	1.49	1.28	25.4	19.7	19.6
HEO	0.16	1.49	1.26	25.4	19.2	17.6
PPO	0.18	1.50	1.79	−25.8	−33.7	−34.3
PBO	0.18	1.50	1.49	−25.8	−25.5	−22.2
MEO	0.76	1.88	1.90	36.2	36.7	41.0
DHO	0.52	1.71	–	31.4	–	37.3

[a]Using the predicted *dr* value. [b]Using the measured *dr* value.

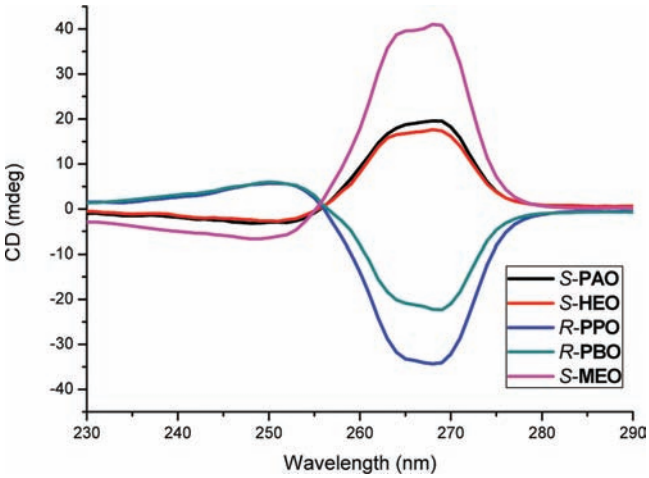

Figure 3. CD spectra of **PAO**-, **HEO**-, **PPO**-, **PBO**-, and **MEO**-derived assemblies in acetonitrile at 25 °C (0.175 mM **2-PA**).

Scheme 6. Alcohols Used for the Prediction of Charton Parameters

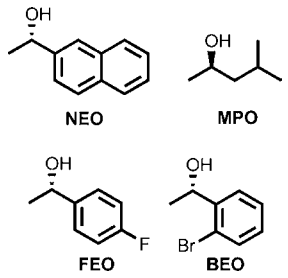

interactions between Br and Me (or OH) in **BEO** make rotation of the C−C bond more difficult, and as a result, the Charton value predicted for 2-bromophenyl (0.77) is closer to the in-plane value of the phenyl group (0.57) than the out-of-plane value (1.66). The result for **BEO** further supports the effect of orientation on the phenyl steric effect as shown in Scheme 4b.

Another interesting example is *R*-4-methyl-2-pentanol (**MPO**), which has methyl and isobutyl (*i*-Bu) groups on the stereocenter. The Charton parameter for *i*-Bu was reported as 0.98, which is larger than that for *i*-Pr (0.76) and *n*-Bu (0.68). However, the *dr* values are 1.23, 1.69, and 1.26 for **MPO** (with *i*-Bu), **MBO** (with *i*-Pr), and **HEO** (with *n*-Bu), respectively. It is reasonable that the steric effect is more sensitive to substitution at the β position of the alcohol, and the aliphatic alcohols with a CH_2 at the β position (**BUO**, **OCO**, **PAO**, **HEO**, and **MPO**) afforded similar *dr* values (1.2−1.3). On the basis of these results, we postulate that *i*-Bu is better modeled using a Charton parameter similar to that for *n*-Bu (0.68).

Scope of the Model. It is worthwhile to discuss the scope and limitations of the quantitative correlations we are proposing to use to predict the CD response. The helical twist is induced by the newly formed stereocenter in the tris(pyridine) complex, which is reflected in the *dr* value, which in turn dictates the sign and magnitude of the first Cotton effect at 268 nm, as previously described. As a result, the *dr*/CD relationship (Figure 1) should be general for all α-chiral secondary alcohols as far as they afford similar amounts of complex **1** in their corresponding multicomponent assembly reactions. However, the $\Delta\upsilon/dr$ correlation (Figure 2) has structural limitations, as do most LFER parameter-based correlations. The alcohols discussed in this paper are either acyclic or cyclic. For acyclic alcohols, there is a methyl on the α carbon, while the other group varies. For cyclic alcohols, there is a hydrogen atom at position 6 of the cyclohexyl ring, while the group at position 2 varies. Hence, the $\Delta\upsilon/dr$ correlation built here applies for α-methyl secondary mono-ols and 2-substituted cyclohexanols. For other mono-ols, such as α-ethyl alcohols, new but similar correlations are likely to be necessary for predictions using steric parameters.

For example, the scope of the linear relationship between the *dr* and the CD magnitude was tested using *S*-1-phenyl-1-propanol (**PRO**; Scheme 7). **PRO** has phenyl and ethyl groups

Scheme 7. Expanded Alcohol Scope for CD Prediction

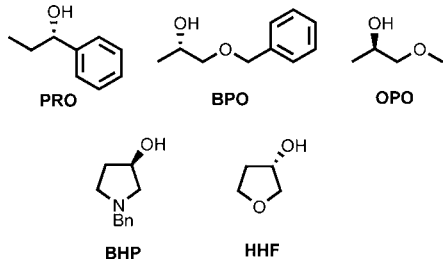

on the stereocenter. ^{1}H NMR spectra revealed that complex **1** was formed with a *dr* value of 1.55. As predicted above, a calculation using the *dr*/CD linear correlation of Figure 1a gave a CD magnitude of 27.1 mdeg at 268 nm, which is close to the experimental value (21.8 mdeg; Figure 4). However, prediction using the sterics-based $\Delta\upsilon/dr$ correlation in Figure 2 was unsuccessful, as reflected in the large difference between the *dr* values for **PRO** (1.55) and **PEO** (2.18).

The ability to predict the CD intensity from the *dr* value of a chiral-alcohol-derived assembly was further expanded to alcohols whose Charton parameters were not previously

dx.doi.org/10.1021/ja3012534 | *J. Am. Chem. Soc.* 2012, 134, 7126−7134

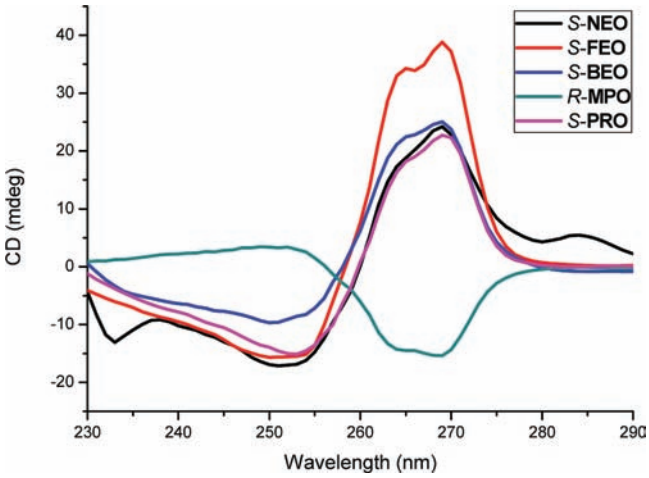

Figure 4. CD spectra of **NEO**-, **FEO**-, **BEO**-, **MPO**-, and **PRO**-derived assemblies in acetonitrile at 25 °C (0.087 mM **2-PA** for **NEO**; 0.175 mM **2-PA** for the other alcohols).

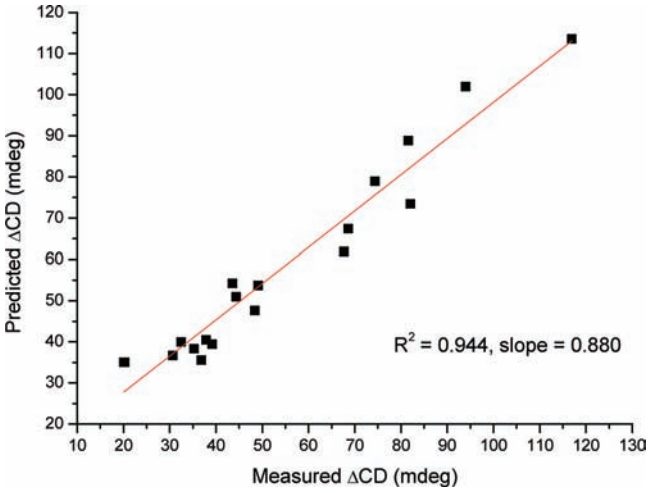

Figure 5. Linear correlation of ΔCD values at 268 nm predicted from measured *dr* values using eq 1 (Figure 1a) with the measured ΔCD values at 268 nm (19 alcohols were used).

reported, as in the cases shown in Scheme 6, as well as heteroatom-containing alcohols (Scheme 7). The prediction of the CD magnitudes using measured *dr* values afforded results comparable to the measured CD values (Table 4 and Figure 4),

Table 4. Prediction of Charton Values and CD Intensities (mdeg) at 268 nm from Measured *dr* Values; the Correlation in Figure 1a Was Used To Predict CD

alcohol	measured *dr*	predicted *υ*	predicted CD	measured CD
NEO[a]	2.42	1.93	51.0	47.0
FEO	2.00	1.44	39.5	37.2
BEO	1.54	0.77	26.8	24.6
MPO	1.23	0.68	−18.3	−15.3
PRO	1.55	–	27.1	21.8
BPO	1.43	–	−23.8	−24.2
OPO	1.29	–	20.0	16.2
HHF	1.20	–	−17.5	−10.0
BHP	1.20	–	17.5	10.1

[a]The CD spectrum was recorded using 0.087 mM **2-PA** because of high absorbance. The measured CD magnitude was doubled for comparison.

although the heteroatom-containing alcohols (**BPO**, **OPO**, **BHP**, and **HHF**) gave CD signals with the opposite sign relative to the other alcohols (see the companion paper for an explanation).

To verify the overall power of the *dr*/CD correlation for all of the alcohols, the ΔCD values at 268 nm predicted from the experimental *dr* values using the correlation in Figure 1a were plotted as a function of the measured ΔCD values. A linear relationship was obtained (R^2 = 0.944, slope =0.880; Figure 5). The correlation in Figure 1b also afforded a linear fit, but with a steeper slope (0.916; see the Supporting Information). This observation is not surprising considering that the relationship in Figure 1b represents reality more closely.

Prediction of *ee* Values. Having successfully predicted *dr* values and CD intensities as well as Charton parameters, we next turned our attention to generating a method for determining *ee* values of chiral alcohols using the linear correlations. Such a method would be important because a calibration curve created from pure enantiomers would not be needed. It is not common to obtain enantiomerically pure *R* and *S* products at the initial stage of an asymmetric reaction and catalyst screen. However, as previously discussed, the *dr* value is independent of the enantiomeric purity (*ee*) of the chiral alcohol and can be commonly obtained by ^{1}H NMR analysis. The comparison of the CD intensity of an assembly formed from an enantiomerically impure alcohol with the predicted CD intensity would therefore allow a quick analysis of the *ee* of the alcohol sample. Moreover, determination of the *ee* for samples used for creating calibration curves and separation of enantiomers could be avoided, thereby further accelerating the reaction screening process.

Several representative alcohols with diverse structures were chosen for *ee* analysis: **PAO**, **PBO**, **MEO**, **NEO**, and **PRO**. The multicomponent assembly reactions were conducted with these alcohols having various *ee* values, and the CD spectra were recorded. The predicted CD intensities at 268 nm were calculated from both measured *dr* values and Charton parameters as appropriate. Because the two enantiomers of a chiral alcohol display equal but opposite CD signals, the ratio of the measured CD magnitude for an alcohol sample to the predicted CD magnitude for an enantiomerically pure sample simply gives the *ee* value. The *ee* values predicted using both methods and the associated absolute errors are listed in Table 5. The calculations using Charton values and measured *dr* values afforded average absolute errors of 13.2 and 9.5%, respectively. The relatively larger error for the Charton-parameter-based prediction is consistent with the similar trend for CD intensity prediction, as listed in Table 3. Irrespective of these errors, it is clear that the *ee* values of a diverse set of chiral secondary alcohols could be determined without the need for either calibration curves or enantioenriched samples to start.

SUMMARY

In summary, LFER-derived Taft-type steric parameters were employed to study *dr* and ECCD properties of a sensing ensemble built from a dynamic multicomponent covalent assembly reaction. The ECCD magnitude resulting from a helical twist induced by the chiral mono-ol is directly correlated with the diastereomeric ratio of the multicomponent assembly. Moreover, models were established to correlate the alcohol

dx.doi.org/10.1021/ja3012534 | J. Am. Chem. Soc. 2012, 134, 7126−7134

Table 5. Prediction of *ee* from Charton Values and *dr* (See Tables 3 and 4 for Predicted Values of *dr* and CD)

alcohol	actual *ee* (%)	CD (mdeg)[a]	predicted *ee* (%)[b]	absolute error (%)	predicted *ee* (%)[c]	absolute error (%)
PAO	−34.0	6.2	−24.5	9.5	−31.6	2.4
PAO	16.0	−1.6	6.3	9.7	8.2	7.8
PAO	100.0	−16.6	65.5	34.5	84.5	15.5
PBO	−46.0	9.5	−36.8	9.2	−37.2	8.8
PBO	10.0	−1.1	4.2	5.8	4.2	5.8
PBO	−76.0	16.8	−65.3	10.7	−66.0	10.0
MEO	53.8	−26.4	72.9	19.1	71.8	18.0
MEO	−18.5	9.2	−25.4	6.9	−25.0	6.5
NEO	63.6	−27.0	–	–	52.9	10.7
NEO	−82.3	33.9	–	–	−66.4	15.9
PRO	10.0	−2.7	–	–	9.9	0.1
PRO	−46.0	9.1	–	–	−33.4	12.6

[a]CD at 268 nm. [b]Predicted using Charton parameters. [c]Predicted using *dr* values measured by ^{1}H NMR spectroscopy.

group size to the *dr* value using Charton steric parameters of the substituents on the alcohol's stereocenter. These two quantitative correlations were used to predict *dr* values and CD magnitudes of several alcohols as well as Charton values of several substituents. Finally, the prediction of enantiomeric purity using both Charton values and measured *dr* values was also achieved, paving the way for quick *ee* analysis.

Previously, the differentiation of enantiomers has been generally achieved through the creation of diastereomers between a chiral host and a chiral guest.[46−48] The variation of enantioselectivity is reflected in the difference of the resulting signals (e.g., NMR integrals or optical responses) for the pair of diastereomers. As a result, a correlation between diastereomer stability (i.e., the sensing signal) and the enantioselectivity of the assay must always exist. In our case, we correlated the CD signal with the *dr* value, which in turn we found to be dictated by steric interactions. Hence, we suspect that correlations with steric parameters are also likely for many other systems that differentiate enantiomers. Therefore, the use of steric correlation models could be a general principle applicable to the development of optical protocols that determine *ee* values. We are currently exploring calculated steric parameters, as well as other classes of chiral substrates, to expand further the scope of sterics-based correlation analysis.

■ ASSOCIATED CONTENT

Supporting Information

Experimental details, spectra data, and additional correlations. This material is available free of charge via the Internet at http://pubs.acs.org.

■ AUTHOR INFORMATION

Corresponding Author

anslyn@austin.utexas.edu

Notes

The authors declare no competing financial interest.

■ ACKNOWLEDGMENTS

We thank the National Institutes of Heath (GM 77437) and the Welch Foundation (F-1151) for financial support.

■ REFERENCES

(1) Reetz, M. T. *Angew. Chem., Int. Ed.* **2001**, *40*, 284−310.
(2) Joyce, L. A.; Shabbir, S. H.; Anslyn, E. V. *Chem. Soc. Rev.* **2010**, *39*, 3621−3632.
(3) Schurig, V. *J. Chromatogr., A* **2001**, *906*, 275−299.
(4) Welch, C. J.; Hyun, M. H.; Kubota, T.; Schafer, W.; Bernardoni, F.; Choi, H. J.; Wu, N.; Gong, X.; Lipshutz, B. *Chirality* **2008**, *20*, 815−819.
(5) Leung, D.; Kang, S. O.; Anslyn, E. V. *Chem. Soc. Rev.* **2012**, *41*, 448−479.
(6) Pu, L. *Chem. Rev.* **2004**, *104*, 1687−1716.
(7) Hembury, G. A.; Borovkov, V. V.; Inoue, Y. *Chem. Rev.* **2008**, *108*, 1−73.
(8) Berova, N.; Di Bari, L.; Pescitelli, G. *Chem. Soc. Rev.* **2007**, *36*, 914−931.
(9) Nieto, S.; Dragna, J. M.; Anslyn, E. V. *Chem.—Eur. J.* **2010**, *16*, 227−232.
(10) Iwaniuk, D. P.; Wolf, C. *J. Am. Chem. Soc.* **2011**, *133*, 2414−2417.
(11) Huang, X.; Fujioka, N.; Pescitelli, G.; Koehn, F. E.; Williamson, R. T.; Nakanishi, K.; Berova, N. *J. Am. Chem. Soc.* **2002**, *124*, 10320−10335.
(12) Kim, H.; So, S. M.; Yen, C. P.; Vinhato, E.; Lough, A. J.; Hong, J. I.; Kim, H. J.; Chin, J. *Angew. Chem., Int. Ed.* **2008**, *47*, 8657−8660.
(13) Leung, D.; Folmer-Andersen, J. F.; Lynch, V. M.; Anslyn, E. V. *J. Am. Chem. Soc.* **2008**, *130*, 12318−12327.
(14) Joyce, L. A.; Maynor, M. S.; Dragna, J. M.; da Cruz, G. M.; Lynch, V. M.; Canary, J. W.; Anslyn, E. V. *J. Am. Chem. Soc.* **2011**, *133*, 13746−13752.
(15) Nieto, S.; Lynch, V. M.; Anslyn, E. V.; Kim, H.; Chin, J. *J. Am. Chem. Soc.* **2008**, *130*, 9232−9233.
(16) Ghosn, M. W.; Wolf, C. *J. Am. Chem. Soc.* **2009**, *131*, 16360−16361.
(17) Shabbir, S. H.; Joyce, L. A.; da Cruz, G. M.; Lynch, V. M.; Sorey, S.; Anslyn, E. V. *J. Am. Chem. Soc.* **2009**, *131*, 13125−13131.
(18) Li, X.; Tanasova, M.; Vasileiou, C.; Borhan, B. *J. Am. Chem. Soc.* **2008**, *130*, 1885−1893.
(19) *Advances in Linear Free Energy Relationships*; Shorter, J., Chapman, N. B., Eds.; Plenum: London, 1972.
(20) Hammett, L. P. *J. Am. Chem. Soc.* **1937**, *59*, 96−103.
(21) Hansch, C.; Leo, A.; Taft, R. W. *Chem. Rev.* **1991**, *91*, 165−195.
(22) Weber, M. E.; Elliott, E. K.; Gokel, G. W. *Org. Biomol. Chem.* **2006**, *4*, 83−89.
(23) Taft, R. W., Jr. *J. Am. Chem. Soc.* **1952**, *74*, 2729−2732.
(24) Taft, R. W., Jr. *J. Am. Chem. Soc.* **1953**, *75*, 4538−4539.
(25) Taft, R. W. In *Steric Effects in Organic Chemistry*; Newman, M., Ed.; Wiley: New York, 1956; pp 556−675
(26) Fujita, T.; Takayama, C.; Nakajima, M. *J. Org. Chem.* **1973**, *38*, 1623−1630.
(27) MacPhee, J. A.; Panaye, A.; Dubois, J.-E. *Tetrahedron* **1978**, *34*, 3553−3562.
(28) Charton, M. *J. Am. Chem. Soc.* **1969**, *91*, 615−618.
(29) Charton, M. *J. Am. Chem. Soc.* **1975**, *97*, 1552−1556.
(30) Charton, M. *J. Am. Chem. Soc.* **1975**, *97*, 3694−3697.
(31) Charton, M. *J. Org. Chem.* **1976**, *41*, 2217−2220.

(32) Winstein, S.; Holness, N. J. *J. Am. Chem. Soc.* **1955**, *77*, 5562−5578.
(33) Bott, G.; Field, L. D.; Sternhell, S. *J. Am. Chem. Soc.* **1980**, *102*, 5618−5626.
(34) Hansch, C.; Leo, A. *Exploring QSAR: Fundamentals and Applications in Chemistry and Biology*; American Chemical Society: Washington, DC, 1995.
(35) Miller, J. J.; Sigman, M. S. *Angew. Chem., Int. Ed.* **2008**, *47*, 771−774.
(36) Sigman, M. S.; Miller, J. J. *J. Org. Chem.* **2009**, *74*, 7633−7643.
(37) Harper, K. C.; Sigman, M. S. *Proc. Natl. Acad. Sci. U.S.A.* **2011**, *108*, 2179−2183.
(38) Harper, K. C.; Sigman, M. S. *Science* **2011**, *333*, 1875−1878.
(39) Rowan, S. J.; Cantrill, S. J.; Cousins, G. R. L.; Sanders, J. K. M.; Stoddart, J. F. *Angew. Chem., Int. Ed.* **2002**, *41*, 898−952.
(40) Corbett, P. T.; Leclaire, J.; Vial, L.; West, K. R.; Wietor, J.-L.; Sanders, J. K. M.; Otto, S. *Chem. Rev.* **2006**, *106*, 3652−3711.
(41) Lehn, J. M. *Chem. Soc. Rev.* **2007**, *36*, 151−160.
(42) Hunt, R. A. R.; Otto, S. *Chem. Commun.* **2011**, *47*, 847−858.
(43) You, L.; Berman, J. S.; Anslyn, E. V. *Nat. Chem.* **2011**, *3*, 943−948.
(44) Galkin, V.; Cherkasov, R. *Org. React.* **1981**, *18*, 113−135.
(45) Galkin, V. I.; Sayakhov, R. D.; Cherkasov, R. A. *Russ. Chem. Rev.* **1991**, *60*, 1617−1644.
(46) Yu, S.; Pu, L. *J. Am. Chem. Soc.* **2010**, *132*, 17698−17700.
(47) Zhu, L.; Zhong, Z.; Anslyn, E. V. *J. Am. Chem. Soc.* **2005**, *127*, 4260−4269.
(48) Mirri, G.; Bull, S. D.; Horton, P. N.; James, T. D.; Male, L.; Tucker, J. H. *J. Am. Chem. Soc.* **2010**, *132*, 8903−8905.